National Defence / Défense nationale

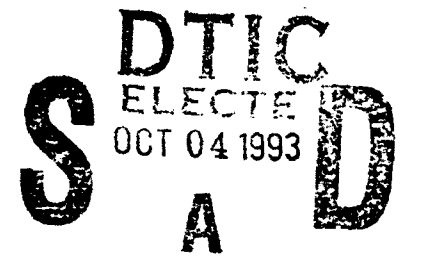

ANALYTIC APPROXIMATIONS OF AN INTEGRAL IN REMOTE SENSING

G.R. Fournier

B.T.N. Evans

RESEARCH AND DEVELOPMENT BRANCH
DEPARTMENT OF NATIONAL DEFENCE
CANADA

BUREAU - RECHERCHE ET DÉVELOPPEMENT
MINISTÈRE DE LA DÉFENSE NATIONALE
CANADA

Defence Research Establishment
Centre de recherches pour la Défense,
Valcartier, Québec

Canada

SANS CLASSIFICATION
DISTRIBUTION ILLIMITÉE

ANALYTIC APPROXIMATIONS OF AN INTEGRAL IN REMOTE SENSING

by

G.R. Fournier and B.T.N. Evans

DEFENCE RESEARCH ESTABLISHMENT

CENTRE DE RECHERCHES POUR LA DÉFENSE

VALCARTIER

Tel: (418) 844-4229

Québec, Canada September/septembre 1993

SANS CLASSIFICATION

ABSTRACT

Approximate analytic solutions to the integrated bistatic signal from Gaussian distributed scatterers in an absorbing medium are derived. Some solutions are useful over limited ranges of the parameters and others are globally more valid. The former are simpler than the latter. The error behaviour of each solution is thoroughly discussed.

RÉSUMÉ

Des solutions approximatives et analytiques sont déterminées pour le problème de l'intégrale du signal bistatique provenant de diffuseurs à distribution gaussienne dans un milieu absorbant. Certaines solutions sont utiles pour des éventails limités de paramètres alors que d'autres sont globalement plus valides. Les premières sont plus simples que ces dernières. Le comportement de l'erreur de chaque solution est discuté en détail.

TABLE OF CONTENTS

EXECUTIVE SUMMARY

The propagation of radiation through Gaussian distributed scatterers in an absorbing medium is a frequently encountered problem. Lidar studies of obscurant or pollution plumes and satellite measurements of biomass in the ocean are two examples. These studies usually try to measure the width and concentration height of Gaussian plumes.

In the above cases, the integrated bistatic signal from remote sensing instruments leads to an integral that cannot be expressed in closed form. In remote sensing applications numerous evaluations of this integral are often required. A great many evaluations of this integral arise when multiple wavelengths, wide area coverage and/or high resolution measurements are involved. Also, a sensitivity analysis may be desired. In addition, the analytic behaviour can provide insight into the problem at hand. Hence, an approximate analytic form would be welcomed.

1.0 INTRODUCTION

Remote sensing applications are increasing rapidly due to the impact of technology. Lidar studies of obscurants and satellite measurements over the ocean are two examples. These applications usually attempt to deduce properties of the scattering medium such as the concentration distribution and attenuation characteristics. Cases where the concentration distribution can be represented by the Gaussian distribution are common. Bistatic scattering from aerosols and hydrosols that are distributed in a Gaussian manner can be analyzed to determine the properties of the distribution remotely. This is highly desirable since these properties determine the input to models that help predict microclimate (obscurants) as well as macroclimate (oceanography) behaviour. The general case must also consider scatterers imbedded in an absorbing medium. This is always the case when studying the biomass of phytoplankton in the ocean and frequently the case with lidar concentration measurements in stack plumes.

This report derives the integral that represents the bistatic return signal from a remote sensing instrument that is staring at scatterers that are Gaussian in their concentration distribution and that are in an absorbing medium. In remote sensing applications numerous evaluations of this integral are often required. A great many evaluations of this integral arise when multiple wavelengths, wide area coverage and/or high-resolution measurements are involved. This is a great computational burden since the integral cannot be expressed exactly in closed form. An approximate analytic form would significantly in-

crease the computational speed and robustness of this integral. Furthermore the analytic behaviour could provide insight into the problem. Hence, an approximate analytic form would be welcomed. (For this report, when we refer to an analytic solution we mean that the result of integration must be represented in terms of combinations of the elementary and special functions of mathematical physics.)

Approximate analytic solutions to this integral are derived. Some solutions are useful over limited ranges of the parameters and others are more globally valid. The former being simpler than the latter. The more globally valid solutions are derived using a new approximation technique (Ref. 1). The error behaviour of each solution is thoroughly discussed.

In Chapter 2.0 the integral is developed. In Chapter 3.0 the various analytic approximations are derived and error behaviour discussed; Chapter 4.0 outlines typical parameters for the lidar and oceanographic cases and Chapter 5.0 gives the conclusions.

This work was performed at DREV between August and September 1992 under PSC 42A, Laser Systems in Support of Military Applications.

2.0 DEVELOPMENT OF THE INTEGRAL

The power received by a bistatic remote sensing instrument P is given by the radar, or lidar equation

$$P = C\sigma_b e^{-2\int_0^z \sigma_e(z')\,dz'}, \qquad [1]$$

where C is a calibration constant depending on the source strength, receiver geometry and distance etc., σ_b is the bistatic or phase function, z is the penetration depth into the scatterers and σ_e is the linear extinction coefficient.

The bistatic function is proportional to the number of scatterers $N(z)$: $\sigma_b = KN(z)$ with K some constant. The extinction coefficient is a sum of two terms, one from the scatterers and one from the absorbing medium, $\sigma_e = k_e N(z) + k_m$ where k_e is the mass extinction coefficient of the scatterers and k_m is the absorption coefficient of the medium.

Since it is assumed that the concentration of the scatterers is a Gaussian distribution superimposed on a constant background, $N(z)$ can be modelled as

$$N(z) = N_o + \frac{N_t}{\sqrt{2\pi}\sigma} e^{-(z-z_m)^2/2\sigma^2}, \qquad [2]$$

where z_m is the peak location, σ defines the width and N_t defines the total concentration of scatterers in the distribution and N_o is the constant background level of scatterers.

The integrated backscatter return is given by the product CKI_1, where

$$I_1 = \int_0^z P\,dz'/CK = \int_0^z N(z')e^{-u(z')}\,dz', \qquad [3]$$

where

$$u(z) = 2\int_0^z [k_e N(z') + k_m]\, dz'. \qquad [4]$$

By using $u'(z) = 2[k_e N(z) + k_m]$, I_1 can be rewritten as

$$I_1 = \frac{1}{k_e}\int_o^z \left[\frac{u'(z')}{2} - k_m\right] e^{-u(z')}\, dz' = \frac{1}{2k_e}\left[e^{-u(0)} - e^{-u(z)} - 2k_m I_2\right], \qquad [5]$$

where

$$I_2 = \int_0^z e^{-u(z')}\, dz'. \qquad [6]$$

Substituting [2] into function $u(z)$, the result can be integrated in closed form as

$$u(z) = 2(N_o k_e + k_m)\, z + \frac{N_t k_e}{2}\left[\mathrm{Erf}\left(\frac{z - z_m}{\sqrt{2}\sigma}\right) + \mathrm{Erf}\left(\frac{z_m}{\sqrt{2}\sigma}\right)\right]. \qquad [7]$$

This equation can then be substituted in [6] and rearranged to give

$$I_2 = \sqrt{2}\sigma e^{-\left[\frac{\alpha z_m}{\sqrt{2}\sigma} + \beta \mathrm{Erf}\left(\frac{z_m}{\sqrt{2}\sigma}\right)\right]} \int_{-\frac{z_m}{\sqrt{2}\sigma}}^{\frac{z - z_m}{\sqrt{2}\sigma}} e^{-[\alpha z + \beta Erf(z)]}\, dz, \qquad [8]$$

where

$$\begin{aligned} \alpha &= 2\sqrt{2}\sigma(N_o k_e + k_m) \text{and} \\ \beta &= N_t k_e/2. \end{aligned} \qquad [9]$$

The integral in [8] cannot be written in closed form in terms of elementary or special functions. Thus the integral to be approximated can be written in generic form as

$$I = \int_0^y e^{-[\alpha z + \beta \mathrm{Erf}(z)]}\, dz = \int_0^y e^{-h(z)}\, dz, \qquad [10]$$

where α and β are positive, y can be positive or negative and $h(z) \equiv \alpha z + \beta \mathrm{Erf}(z)$.

3.0 ANALYTIC APPROXIMATIONS

This chapter will derive and discuss analytic approximations with various ranges of validity. These approximations are obtained by using several different techniques.

3.1 Small y

For small y the Error function, $\mathrm{Erf}(z)$, can be expanded in powers of z. Keeping only the first order term, [10] becomes

$$\begin{aligned} \lim_{y \to 0} I &= \int_0^y e^{-s\,z}\,dz \\ &= \frac{1}{s}\left[1 - e^{-s\,y}\right] \end{aligned} \qquad [11]$$

where

$$s = \alpha + \frac{2}{\sqrt{\pi}}\beta. \qquad [12]$$

Figure 1 is a contour diagram of absolute relative error between [11] and I for $\alpha = 0$. The maximum error in computing I by [11] occurs when $\alpha = 0$ since larger α reduces the relative error in the exponential coefficient. The error is not symmetrical in y. For $y > 0$ the error is less since [11] can also be derived under the conditions of large β and $y > 0$. This can be easily shown. When β is large, the major contribution to I comes from small y. This idea is identical to the concept behind Laplace's method of steepest descent given in the next section.

Another approach is to do a variable substitution in [10] for $h(z)$ and then approx-

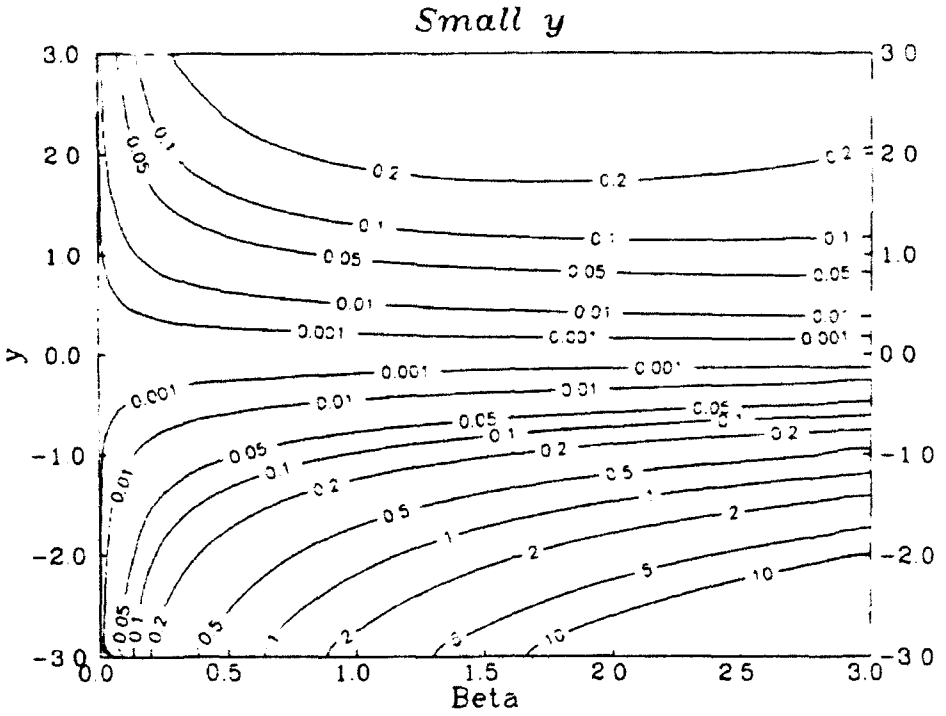

FIGURE 1 – Contour diagram of absolute relative error for the small y approximation

imate its inverse function for small y. The first order result is the same as [11]. The second order is

$$\lim_{y\to 0} I = \frac{1}{s}(1+\frac{2\beta}{\sqrt{\pi}s^3})(1-e^{-h(y)}) - \frac{2\beta h(y)}{\sqrt{\pi}s^4}e^{-h(y)}. \qquad [13]$$

This approximation is more complicated than [11], and only marginally improves the error for small y.

3.2 Large β, $y > 0$

When β and sy become large, Laplace's method of steepest descents can be used to obtain the asymptotic limit of I. Using this method to second order (Ref. 2) the limit is

$$I_s \equiv \lim_{\beta->\infty} I = \frac{1}{s}\left[1+\frac{4\beta}{\sqrt{\pi}s^3}\right]. \qquad [14]$$

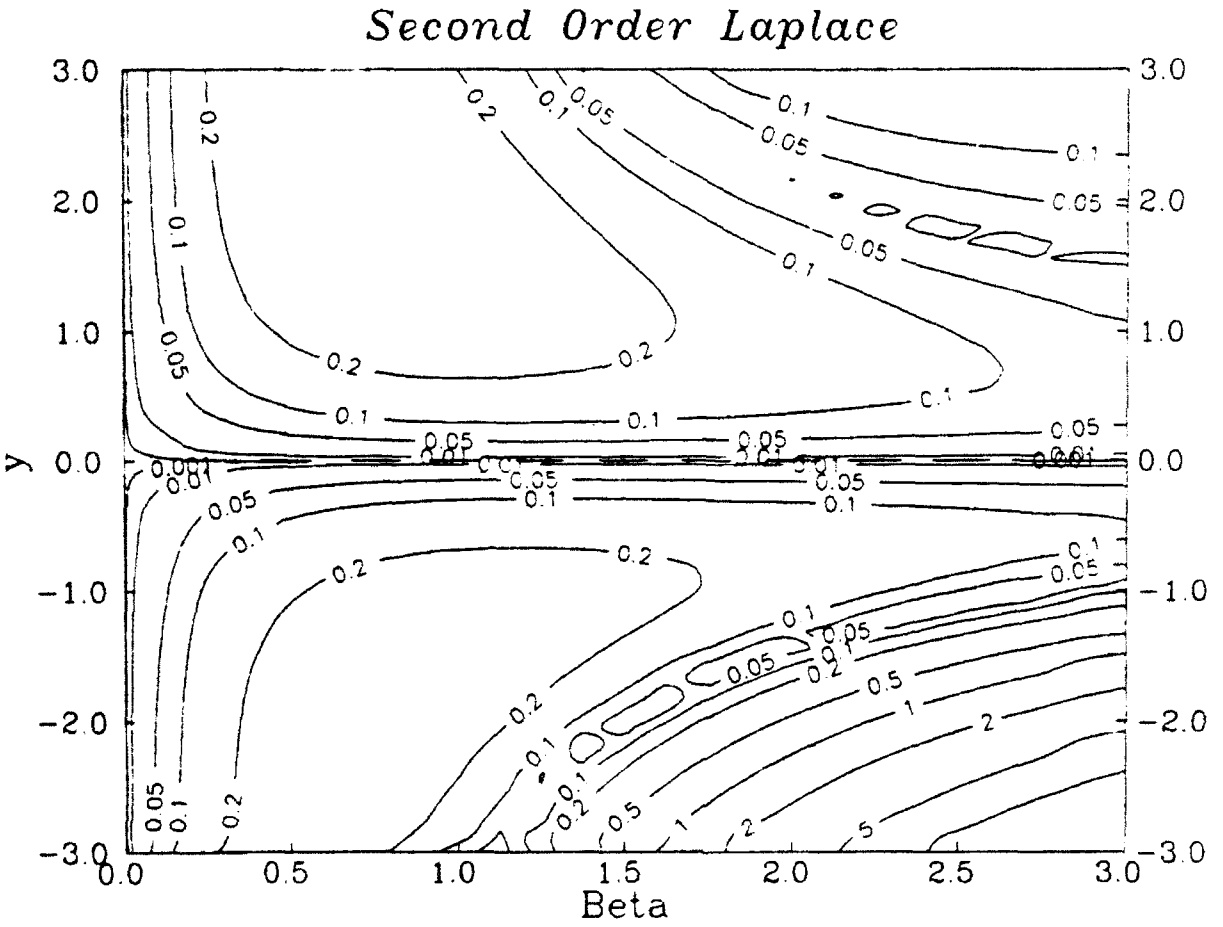

FIGURE 2 – Contour diagram of absolute relative error for the large β, $y > 0$ approximation

The first term in [14] is identical to the first term in [11]. Furthermore, [11] does not have the second constraint, sy being large due to the exponential term. Therefore the following *Ansatz* is the most natural:

$$\lim_{\beta \to \infty} I = I_s(1 - e^{-y/l_s}). \qquad [15]$$

Figure 2 is a contour diagram of absolute relative error between [15] and I for $\alpha = 0$. It has been computed for $y < 0$, as in Fig. 1, for comparison and as an indication of the full range of validity of [15]. Figure 2 shows that [15] is an improvement over [11] for large β and $y > 0$. It should be noted that [15] is a much better aproximation than [14] when $sy < 3$.

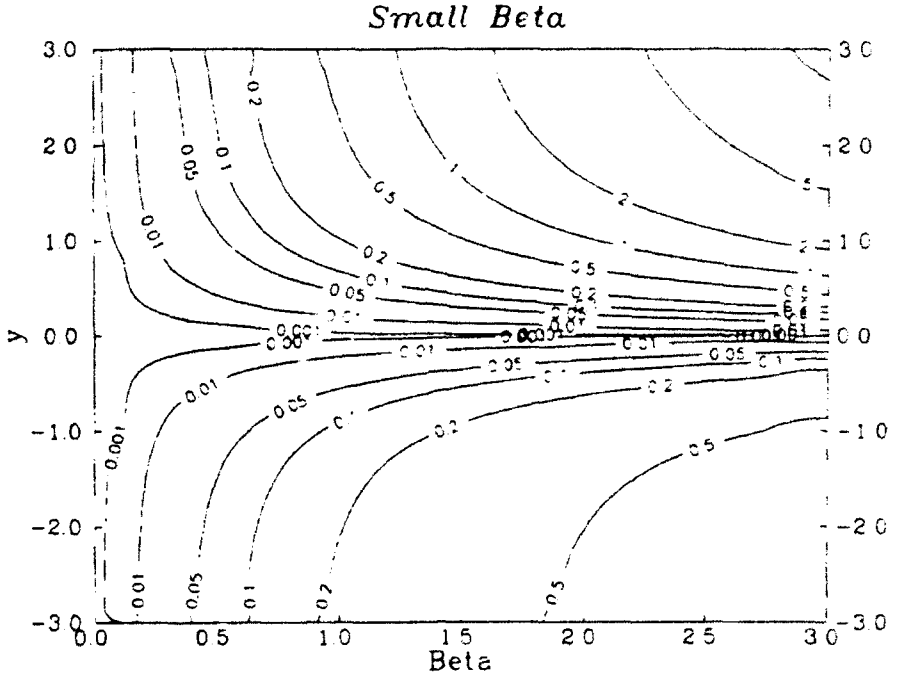

FIGURE 3 - Contour diagram of absolute relative error for the small β approximation

3.3 Small β

If β is small enough, a simple expansion of $e^{-\beta \mathrm{Erf}(z)}$ in β can be done. Only the first two terms of this expansion can be kept in order to obtain closed form expressions. Doing this the approximation becomes

$$\lim_{\beta \to 0} I = \frac{1}{\alpha} \left[1 - e^{-\alpha y} - \beta \left\{ e^{\alpha^2/4} \left[\mathrm{Erf}(y + \alpha/2) - \mathrm{Erf}(\alpha/2) \right] - e^{-\alpha y} \mathrm{Erf}(y) \right\} \right]. \qquad [16]$$

The corresponding absolute relative error diagram is shown in Fig. 3.

If the kernel of I is approximated by Chebyshev polynomials (Ref. 3), the absolute error in the kernel is then minimized. This leads to the approximation

$$\lim_{\beta \to 0} I = \frac{1}{\alpha} \left[c_0 (1 - e^{-\alpha y}) - c_1 \left\{ e^{\alpha^2/4} \left[\mathrm{Erf}(y + \alpha/2) - \mathrm{Erf}(\alpha/2) \right] - e^{-\alpha y} \mathrm{Erf}(y) \right\} \right],$$

$$c_0 = e^{-c/2} (I_0[c/2] + 2 I_1[c/2])$$

$$c_1 = 4I_1[\beta/2], \qquad [17]$$

with $c = \beta \mathrm{Erf}(y)$. In [17], I_0 and I_1 are the zero and first order modified Bessel functions of the first kind.

This approximation, however, does not provide the best error in I. If the kernel is instead approximated by a minimax procedure, the absolute relative error is minimized. Unfortunately, this must be done numerically and thus good approximations to the coefficients must be found. The numerical procedure, MiniMax, found in Mathematica (Ref. 4) was used. The resulting coefficients were empirically fitted.

$$\begin{aligned}
\lim_{\beta \to 0} I &= \frac{1}{\alpha}\left[c_0(1-e^{-\alpha y}) - c_1\left\{e^{\alpha^2/4}\left[\mathrm{Erf}(y+\alpha/2) - \mathrm{Erf}(\alpha/2)\right] - e^{-\alpha y}\mathrm{Erf}(y)\right\}\right], \\
c_0 &= J_0[c/2] \\
c_1 &= e^{-c/2-(c/7)^2} \quad \text{for } y > 0 \\
&= e^{-c/2} \quad \text{for } y < 0, \qquad [18]
\end{aligned}$$

where J_0 is the zero order Bessel function of the first kind. The error diagram is shown in Fig. 4. It is clear that [18] is superior to [16]. Worst errors, which occur as $y \to \infty$, are 0.06 % for $\beta = .1$, 0.5 % for $\beta = .3$, 6.25 % for $\beta = 1$ and 34 % for $\beta = 2$.

3.4 Kernel Approximation

The partial kernel $e^{-\beta \mathrm{Erf}[z]}$, can be approximated by modelling its behaviour in the range $z \to 0$ and $z \to \infty$. At $z = 0$ it is 1, at $z = \infty$ it is $e^{-\beta}$ and at $z = -\infty$ it is e^{β}. This

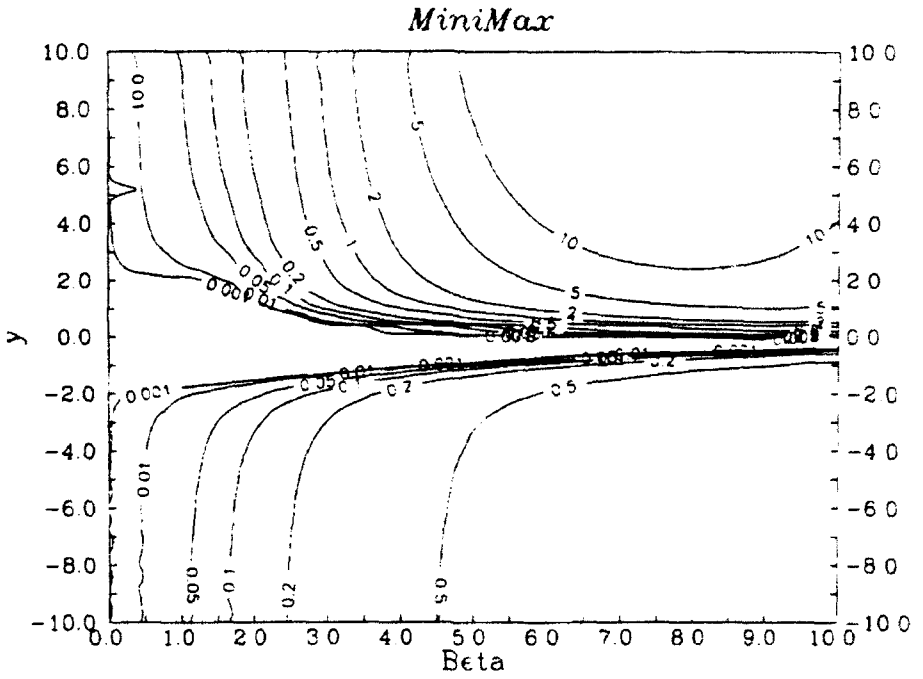

FIGURE 4 – Contour diagram of absolute relative error for the minimax approximation.

suggests the following interpolation:

$$e^{-\beta \mathrm{Erf}[z]} \approx e^{\mp\beta} + (1 - e^{\mp\beta})e^{-\delta z}, \qquad [19]$$

where it is understood that the upper minus sign is used when $z > 0$ and the lower plus sign when $z < 0$. In the above δ can be found by assuming that it is independent of z and simplifying [19] by letting $z \to 0$. This gives

$$\delta = \frac{2}{\sqrt{\pi}} \frac{\beta}{1 - e^{\mp\beta}}. \qquad [20]$$

Integrating to obtain I, with the kernel approximated by [19], gives

$$I \approx \frac{e^{\mp\beta}}{\alpha}[1 - e^{-\alpha y}] + \frac{(1 - e^{\mp\beta})}{\alpha + \delta}\left[1 - e^{-(\alpha+\delta)y}\right]. \qquad [21]$$

This gives a remarkably simple approximation to I when $y > 0$. The error diagram, given by Fig. 5, shows that it is a very good approximation. The worst error is 5.77 % when

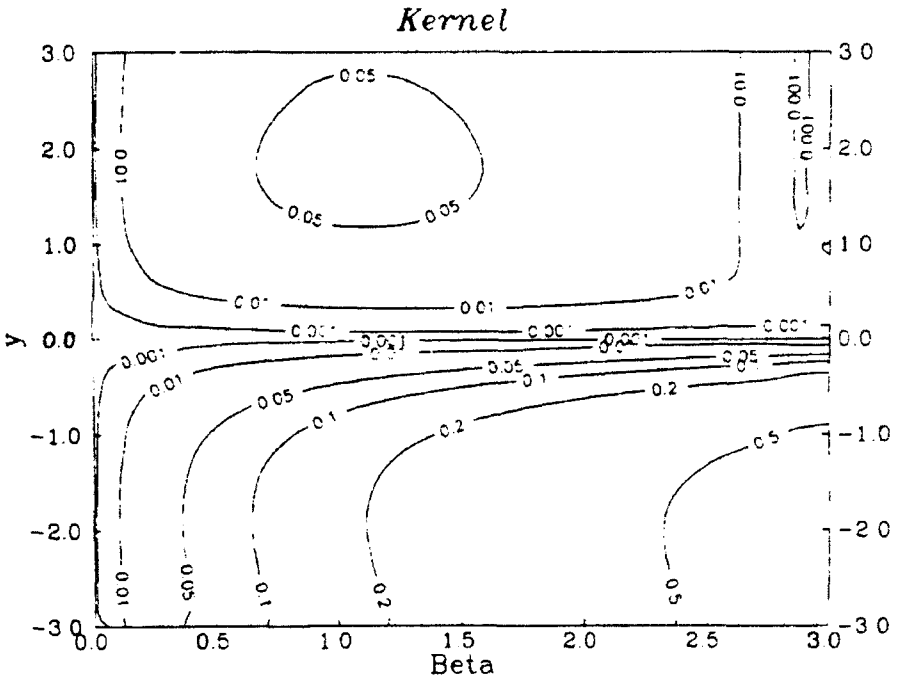

FIGURE 5 – Contour diagram of absolute relative error for the kernel approximation

$\alpha = 0$, $\beta = 1.09$ and $y = 1.70$. Obvious simple extensions, such as the addition of another exponential term in [19], or replacing δx by $\delta x + \epsilon x^2$, either do not work or produce solutions that are much less accurate.

3.5 Analytic Approximation Technique

The next two sections apply the approximate analytic technique Ref. 1 to obtain two additional analytic approximations to I.

3.5.1 Exponential Integral Solution

The integration technique of (Ref. 1) can be readily applied to I. This technique is essentially an approximate change of variables. This procedure can be applied to an integral

such as

$$Q = \int_0^y e^{h[z]} f[z]\, dz, \qquad [22]$$

where $h[z]$ is an arbitrary function, but usually roughly monotonic, and $f[z]$ is a function that is relatively easy to integrate in closed form. Then Q is approximated by

$$Q \approx \int_{h[0]}^{h[y]} e^h u[h]\, dh, \qquad [23]$$

where $h[z]$ has now become the dummy variable and $u[h]$ satisfies the two constraints

$$u[h]\, dh \approx f[z]\, dz \qquad [24]$$

over the range of interest, and the integral in [23] can be evaluated in closed form.

In the case of I, $\alpha z + \beta \mathrm{Erf}(z)$ can be identified with $h[z]$ and $f[z] = 1$. A functional form for $u[z]$ that satisfies the closed form constraint is $q_1(z + q_2)^d$, where q_1, q_2 and d are parameters. These are found by satisfying [24]. This functional form, which is the binomial function, can be designed to have $u[h]\,dh$ fit $f[z]\,dz$ at three points with the correct curvature. The curvature is decided by d. For the present case $d = 2$ is found to be optimal. See Ref. 1 for more details. Doing the appropriate algebra, we see that the final solution for this approximation is

$$I \approx q_1 e^{q_2} \left[\frac{E_2(h[y] + q_2)}{h[y] + q_2} - \frac{E_2(q_2)}{q_2} \right], \qquad [25]$$

where

$$q_1 = -q_2 q_3,$$

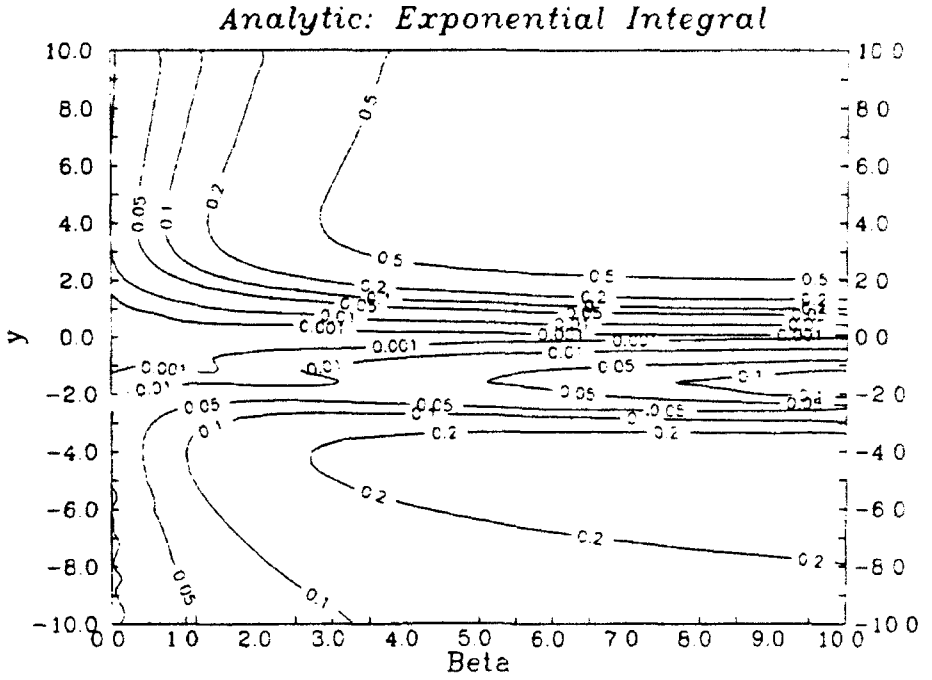

FIGURE 6 – Contour diagram of absolute relative error for the exponential integral approximation

$$q_2 = \frac{h[y/2]h[y]}{h[y] - 2h[y/2]}$$
$$q_3 = y\frac{h[y] + q_2}{h[y].} \qquad [26]$$

The error diagram is shown in Fig. 6. The error increases as $|y|$ and/or β increase. However, when $|y|$ is large, $\mathrm{Erf}[y] \approx 1$ and hence I can be split into the sum of two integrals. This possibility will be discussed in the next section and this procedure will be seen to result in a much improved solution.

3.5.2 Exponential Solution

Applying the integration technique as in the last subsection but using the exponential function for $u[h]$ instead of the binomial function, a different solution is obtained.

Thus, $u[h] = q_1 e^{q_2 h}$. Also, for ease of notation, $h[z] = \mathrm{Erf}[z] + \gamma z$, where $\gamma = \alpha/\beta$.

The one additional complication in obtaining this solution is that an implicit equation must be solved. This equation is a result of fitting the differential $u[h]\,dh$ to the differential $f[z]\,dz$ at three points, whereas in the previous solution the fitting parameters could be solved explicitly. This equation is

$$\frac{y}{y/a} = a = \frac{e^{q_1 h(y)} - 1}{e^{q_1 h(y/a)} - 1}, \qquad [27]$$

where a determines the location of the middle fitting point, y/a, in the interval $[0, y]$. The approximate analytic solution to this equation can be found by taking the various limits of its parameters and solving. First, let $\alpha = 0$ and take the two limits of q_1, one as $y \to 0$ and the other as $y \to \infty$. One synthetic equation can be written that satisfies both limits and achieves reasonable accuracy in the intervening region:

$$q_1[\alpha = 0] \approx \frac{\sqrt{\pi}}{3a} \frac{(1+a) y e^{y^2} \ln(a)}{e^{(1-\frac{1}{a^2})y^2} + \ln(a) - 1}. \qquad [28]$$

Using the above solution, valid for small α, an equation satisfying both limits of y and arbitrary α can be obtained by using the same synthetic technique:

$$q_1 \approx \frac{4(1+a)\sqrt{\pi}\ln(a) y e^{y^2}}{3a(2+\gamma\sqrt{\pi})^2(e^{(1-\frac{1}{a^2})y^2} + \ln(a) - 1) + \sqrt{\pi}\gamma y^2 e^{y^2}(1+\gamma y)\ln(a) 2(1+a)/a}. \qquad [29]$$

With the approximate solution for q_1 we can estimate q_2 as

$$q_2 = \frac{y q_1}{e^{q_1 h(y)} - 1}. \qquad [30]$$

With these parameters, and setting $a = 2$ the approximation to I becomes

$$I \approx q_2 \int_0^y e^{-\beta h} e^{q_1 h}\, dh$$

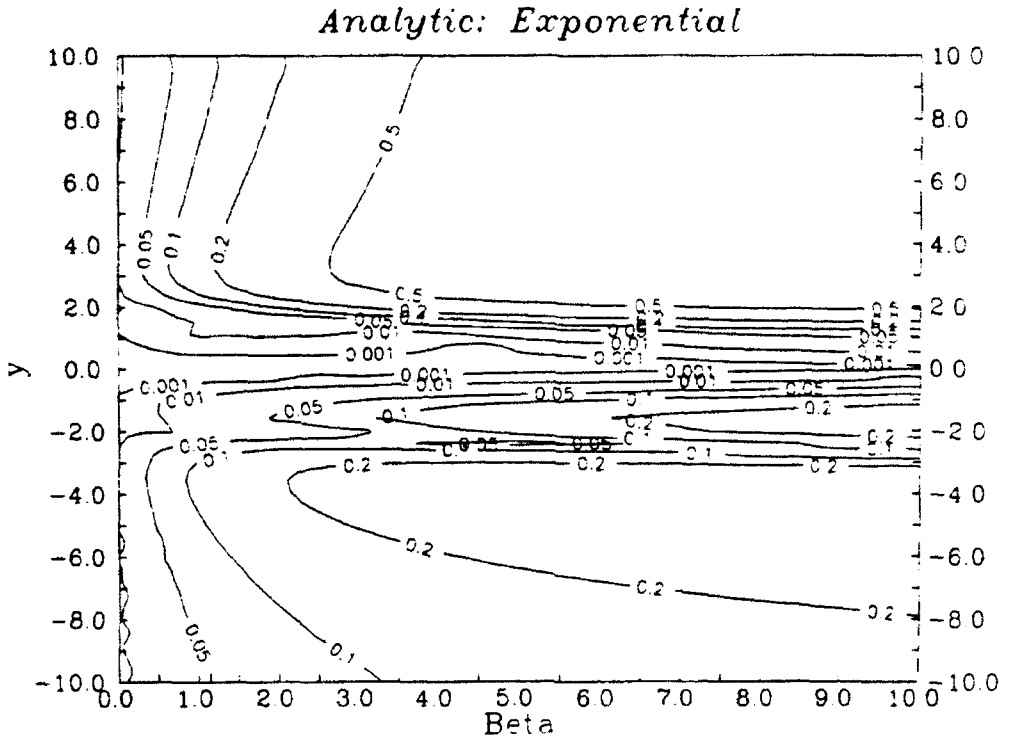

FIGURE 7 – *Contour diagram of absolute relative error for the exponential approximation*

$$= \frac{q_2}{q_1 - \beta}\left[e^{(\alpha y+\beta \mathrm{Erf}[y])(q_1/\beta-1)} - 1\right]. \qquad [31]$$

Figure 7 is the absolute relative error diagram for this approximation. This shows similar behaviour to that of the previous approximation. Once again, I can be split into the sum of two integrals. The next section will make it clear why this analytic technique is of value.

3.6 Splitting the Integral

All of the approximations in the previous section have one or more regions where the error is unacceptably large. In cases where these errors occur at large magnitudes of y. (about $y > 2$) the integral can be split into two. This is done by assuming that, for large

enough y, $\beta \mathrm{Erf}[y] \approx \beta y/|y|$. Hence,

$$I = \int_0^{y_m} e^{-\alpha z - \beta \mathrm{Erf}[z]}\, dz + \frac{e^{-\beta y/|y|}}{\alpha}(e^{-\alpha y_m} - e^{-\alpha y}), \qquad [32]$$

where y_m is the splitting function. This splitting of the integral will work best in conjunction with the approximations that have the smallest errors at the largest magnitudes of y. Inspection of Figs. 1-7 indicates that the only two suitable candidates are the exponential and exponential integral solutions. The immediate problem is to find an optimum y_m. As there is no evident theoretical approach to finding y_m, it is easiest to determine it empirically. From the error diagram behaviour of the two analytic approximations, Figs. 6 and 7, it is clear that y_m has a different behaviour if $y > 0$ than if $y < 0$. For $y > 0$, y_m decreases with β and for $y < 0$, y_m increases with β.

For both analytic approximations the split function has been empirically determined. It is for $y > 0$,

$$\begin{aligned} y_m &= (1-p)(1.252 - .026(\alpha+\beta)) + 3.08629p/(8+\alpha+\beta)^{.81078} \\ p &= (\alpha+\beta)^3/(9^3+(\alpha+\beta)^3). \end{aligned} \qquad [33]$$

For $y < 0$ it is

$$\begin{aligned} y_m &= -2, \qquad \beta \le e \\ &= \sqrt{2\ln\left[\frac{\beta^2}{\ln[\beta]}\right]}, \qquad \beta > e. \end{aligned} \qquad [34]$$

Using this split function and approximating the integral in [32] by the exponential integral solution, or the exponential solution, error diagrams can be computed. The results are

shown in Figs. 8 and 9, respectively. Now, the asymptotic error in y is handled correctly for both $y > 0$ and $y < 0$ in both approximations. The remaining problem area, for $y \approx -2$ and $\beta > 2$ cannot be gotten rid of without further splitting the integral and performing additional approximations such as expansion of Erf[z] about $y \approx -2$. Even this yields only a marginal improvement at the cost of significant complexity. The center of the problem area is asymptotically determined by

$$y \asymp \mathrm{Erfc}^{-1}\left[\frac{1}{\sqrt{\pi}\beta}\right] \approx \sqrt{\frac{1}{2}\ln\left[\frac{\beta^2}{\ln[\beta]}\right]}. \qquad [35]$$

This region gives the worst errors for both approximations when $\alpha = 0$ and for about $\beta > 4$. Over the range of β covered by Figs. 8 and 9, the worst error occurs at $\beta = 10$. For the exponential integral approximation when $y = -1.72$ it is 14.3%, and for the exponential approximation when $y = -1.77$ it is 30.5%.

4.0 APPLICATIONS

In this section, two practical applications of the approximations will be considered. This is to focus attention on the ranges of α and β that are likely to be encountered. The range of these parameters obviously influences the choice of approximation. The two applications involve lidar and remote sensing of oceanic biomass.

Table I summarises values of the input parameters required to calculate α, β and y for typical lidar results in obscurants and remote sensing of oceanic biomass. The lidar parameters were taken from Ref. 5 and Ref. 7. The oceanic biomass parameters were

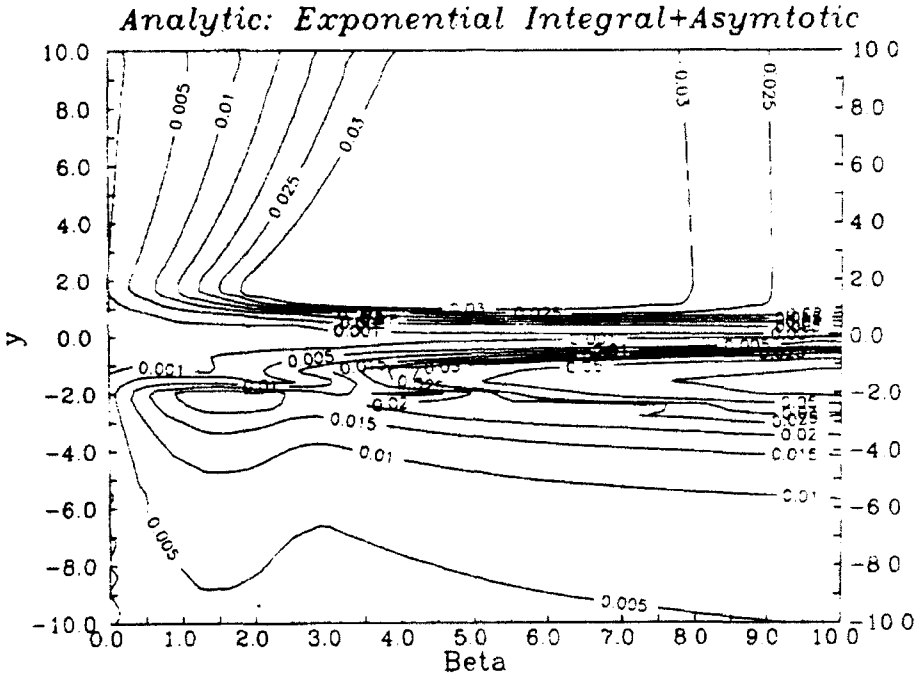

FIGURE 8 – Contour diagram of absolute relative error for the split exponential integral approximation

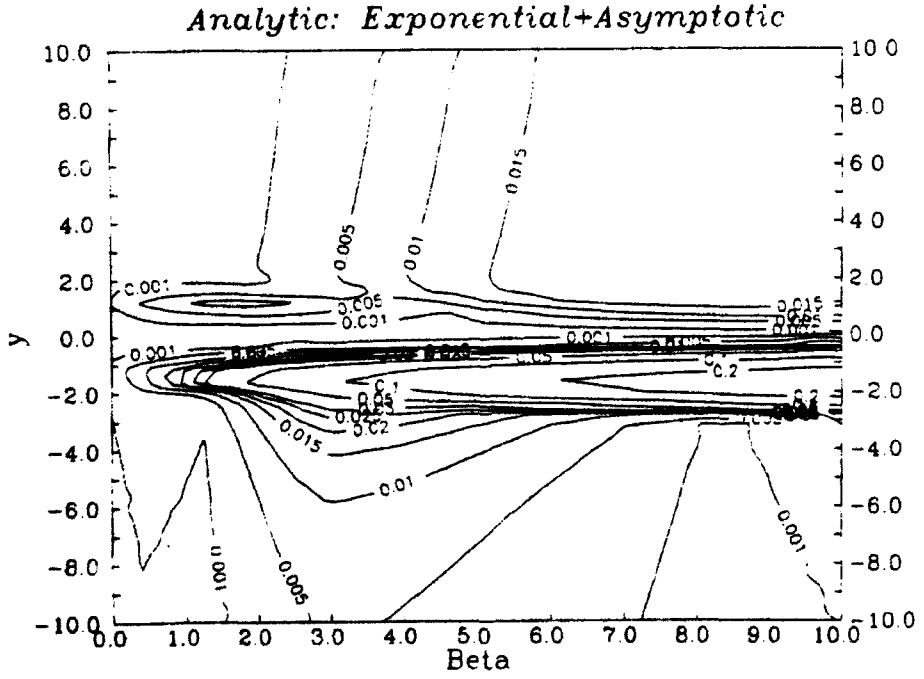

FIGURE 9 – Contour diagram of absolute relative error for the split exponential approximation

TABLE I

Lidar and Oceanic Parameters

Parameters	Lidar	Oceanic
N_o g/m^3	2×10^{-5}	10^{-4}
N_t g/m^2	5	$0.0188/c^*$
k_e m^2/g	1	$20c^*$
k_m 1/m	5×10^{-6}	.02
σ 1/m	20	5
z_m m	500	42.5
α	0.40	0.30
β	2.5	0.15
y	$-20 < y < 2$	$-6 < y < \infty$

* c is the ratio of chlorophyll mass to phytoplankton mass

obtained from Ref. 6. Note that the ratio of chlorophyll mass to phytoplankton mass, c, is not needed to obtain the derived parameters since it drops out.

The following discussion is made simplest if we assume y is arbitrary and α arbitrary positive. From the error diagrams the critical parameter is the magnitude of β. When β is small, as in the oceanic case, a number of approximations, discussed in the previous chapter, can be used. For this case where β is typically 0.15, the kernel approximation [21] is the simplest and gives worst errors of about 1 %. Values of β up to 0.4 can be accommodated with errors less than 5 %. The next simplest approximation with improved accuracy is the

TABLE II

Accuracy Guide

Approximation	1%	5%	10%	20%
Small β [16]	0.1	0.3	0.5	0.9
Kernel [21]	0.1	0.4	0.6	1.1
MiniMax [18]	0.4	0.7	1.0	1.5
Split Exponential [31,32]	0.5	1.7	3.2	6.0
Split Exponential Integral [25,32]	0.3	5.0	7.7	14.0

minimax approximation [18]. Errors of less than 5 % occur for $\beta < 0.7$.

For typical lidar scenarios in obscurants or smoke stacks β is about 2.5, which is considerably larger than in the oceanic case. If errors of less than 5 % are required only one approximation can be used, the split exponential integral approximation. If y is never close to where the maximum error occurs (at typically $y \approx -2$), then other approximations can be considered. Indeed, since lidar is a remote sensing instrument, y usually ranges from small positive values to large negative values. In this case combinations of the kernel approximation with the asymptotic solution for $y < 0$ may be excellent.

Table II is a condensed guide of the recommended approximations. It lists the highest β that can be used for a given level of accuracy. This accuracy level is approximately the worst error for arbitrary y and α.

Values of β can, under extreme circumstances, be over an order of magnitude higher than the typical values given in Table I. These may occur near the smoke source in the case of obscurants or smoke stacks, or in dense plankton blooms. In addition, sensitivity analysis may require higher values of β than can be expected realistically. However, the task at hand is usually to determine the three derived parameters, α, β and y and from them the physically interesting quantities. This requires an inversion of the integral. The errors incurred in estimating the three derived parameters by inversion of the approximations can be quite different from the error behaviour outlined in the diagrams or Table II. An example of this is given in Fig. 10. The split exponential integral approximation was used to find β given the integral

$$I_d = I[y_u] - I[y_l] = \int_{y_l}^{y_u} e^{-\alpha z - \beta \mathrm{Erf}[z]} dz, \qquad [36]$$

which is related to I_2, [8]. In Fig. 10, $\alpha = 0$ and $y_u = 10$. The inversion was performed by minimizing the absolute relative difference between I_d at a fixed β and its approximation with varying β. It can be seen that the pattern of error is quite different from the error diagram for this approximation, Fig. 8. This is because the error in the inversion can be more sensitive to the change in the value of the integral as β changes than the error of the approximation

$$\delta\beta = \frac{\partial \beta}{\partial I_d} \delta I_d. \qquad [37]$$

Here, $\delta\beta$ and δI_d represent the error in β and I_d respectively. In Fig. 10 the worst error is about 15 %.

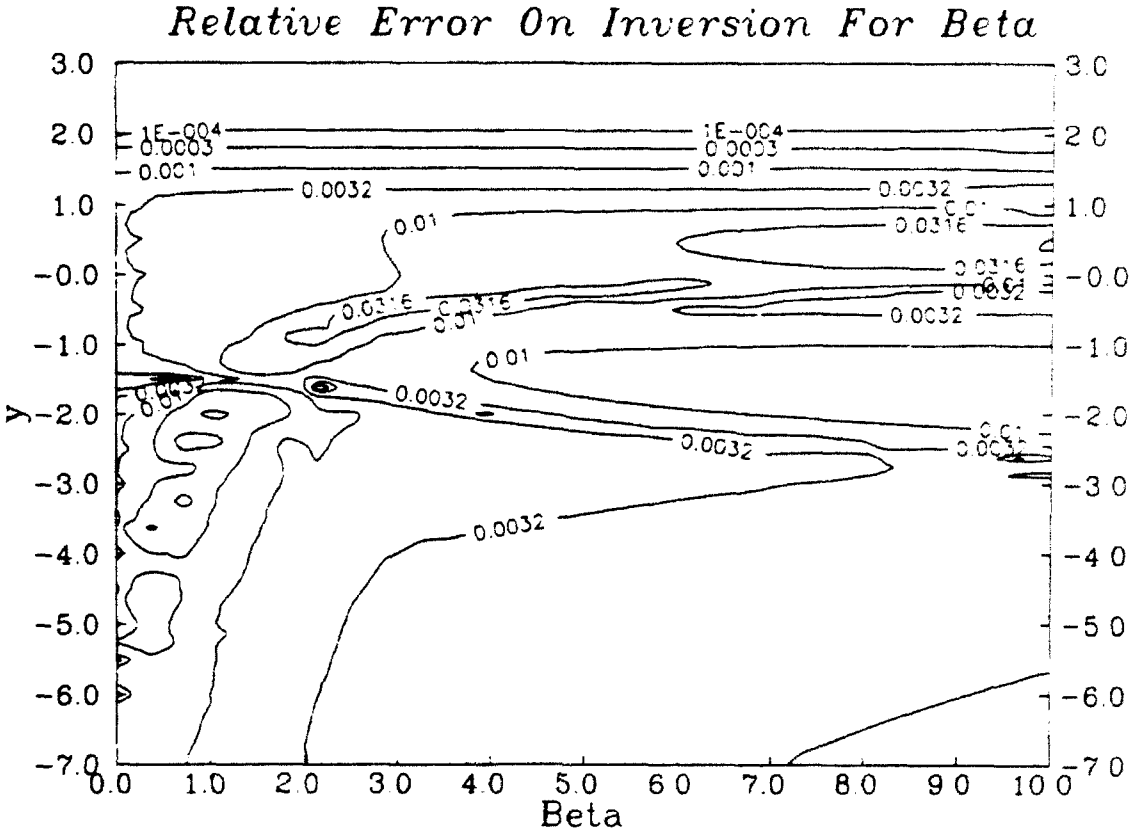

FIGURE 10 - Contour diagram of absolute relative error on inversion for β

5.0 CONCLUSIONS AND DISCUSSION

Seven analytical approximations to the integrated bistatic signal from Gaussian-distributed scatterers were derived. The error behaviour of each solution was thoroughly discussed. Four of these, not including some related approximations, were derived based on well-known approaches. The other three use more nonstandard techniques.

The approximations allow for trade-offs between analytic simplicity and accuracy. Furthermore, the effects of the error in the approximation on the inversion of the integrated signal to estimate the parameters involved was found to be minor. This implies that some of the approximations can be used to determine the *in situ* parameters from remote sensing data.

The analytic nature of the approximations allows for rapid evaluation of the integral and can lead to additional insight.

6.0 REFERENCES

1. Evans, B.T.N. and Fournier, G.R., "A Procedure for Obtaining an Algebraic Approximation to Certain Integrals", DREV R-4653/91, August, 1991, UNCLASSIFIED.

2. Pearson, C.E., "Handbook of Applied Mathematics: Selected Results and Methods", Van Nostrand Reinhold Co., Second Edition, New York, 1983.

3. Luke, Y.L., "The Special Functions and Their Approximations", Vols. I and II, Academic Press, New York, 1969.

4. Wolfram, S., "Mathematica: A System for Doing Mathematics by Computer", Addison-Wesley, New York, 1989.

5. Evans, B.T.N. and Roy, G., "Comparison of the Laser Cloud Mapper and Nephelometer Aerosol Concentration Data Taken at Smoke Week IX", DREV R-4576/89, December, 1989, UNCLASSIFIED.

6. Sathyendranath, S. and Platt, T, "Remote Sensing of Ocean Chlorophyll: Consequence of Nonuniform Pigment Profile", Applied Optics, Vol. 28, pp.490-495, February, 1989.

7. Wolfe, W.L. and Zissis, G.J., "The Infrared Handbook", Office of Naval Research, Dept. of the Navy, Washington, D.C., 1978.

INTERNAL DISTRIBUTION

DREV R-4724/93

1 – Deputy Chief
1 – Director Electro–optics Division
1 – Director Energetic Materials Division
6 – Document Library
1 – Dr. G.R. Fournier (author)
1 – Dr. B.T.N. Evans (author)
1 – Dr. P. Pace
1 – Dr. L. Bissonnette
1 – Mr. D. Hutt
1 – Dr. P. Roney
1 – Dr. G. Otis
1 – Mr. R. Kluchert
1 – Mr. G. Roy (Energetic Materials)
1 – Mr. G. Couture

EXTERNAL DISTRIBUTION

DREV R-4724/93

2 - DSIS
1 - CRAD
1 - DRDL
1 - DRDM
1 - National Library of Canada
1 - Micromedia Limited
1 - NRC/CISTI
1 - DRIC, U.K.
1 - DTIC, U.S.
1 - DISSLB, Australia

1 - Dr. A.I. Carswell
Dept. of Physics
York University
4700 Keele Street
North York, Ontario
M3J 1P3

1 - Dr. T. Platt
Biological Oceanography Division
Department of Fisheries and Oceans
Bedford Institute of Oceanography
P.O. Box 1006
Dartmouth, N.S. B2Y 4A2